Nephrol Dial Transplant (2008) 23: 525–533
doi:10.1093/ndt/gfm547
Advance Access publication 23 November 2007

Original Article

NDT
Nephrology Dialysis Transplantation

Venous stenosis in a pig arteriovenous fistula model—anatomy, mechanisms and cellular phenotypes*

Yang Wang[1], Mahesh Krishnamoorthy[2], Rupak Banerjee[2], Jianhua Zhang[1], Steven Rudich[3], Christy Holland[4], Lois Arend[5] and Prabir Roy-Chaudhury[1]

[1]Cincinnati Dialysis Access Research Program, Department of Medicine, Division of Nephrology, [2]Department of Mechanical, Industrial and Nuclear Engineering, [3]Department of Surgery, [4]Department of Biomedical Engineering and [5]Department of Pathology, University of Cincinnati, Cincinnati, OH, USA

Abstract

Background. Haemodialysis vascular access dysfunction is currently a huge clinical problem. Although arteriovenous (AV) fistulae are the preferred mode of dialysis access, they have significant problems with both early (failure to mature) and late fistula failure. Both are characterized radiologically as a stenosis of the venous segment. Despite the magnitude of the clinical problem, the exact pathogenesis of AV fistula failure remains unclear. The aim of this study was to develop and validate a pig model of AV fistula stenosis and then use it to dissect out the mechanisms responsible for this lesion.

Methods. AV fistulae were created between the femoral artery and vein of Yorkshire Cross pigs. Animals were sacrificed at 2 days, 7 days, 28 days and 42 days post-surgery. At the time of sacrifice the entire specimen was divided into four regions; the arterial (AV-A) and venous (AV-V) portions of the AV anastomosis, the juxta-anastomotic segment (JA) and the proximal vein (PV), and assessed for the degree of intima-media thickening and the presence of specific cellular phenotypes. Haemodynamic parameters were not measured in this set of experiments.

Results. Significant luminal stenosis and intima-media thickening were present as early as 28 days and 42 days post-surgery in the pig model. In addition, within specimens from a single time point, these two parameters were maximal within the proximal vein and juxta-anastomotic segment as compared to the AV anastomosis ($P < 0.0001$). The vast majority of cells within the region of intima-media thickening were myofibroblasts.

Conclusions. These studies suggest that early and aggressive intima-media thickening (which is made up primarily of myofibroblasts) plays an important role in AV fistula stenosis in a pig model of AV fistula placement. Interventions that target the mechanisms and cellular phenotypes described in this model, may be effective in reducing the very significant morbidity and economic costs currently associated with AV fistula failure.

Keywords: arteriovenous fistula stenosis; cellular phenotypes; hemodialysis vascular access dysfunction; myofibroblast; neointimal hyperplasia; pig model

Introduction

In an attempt to reduce the very significant morbidity and economic cost associated with haemodialysis vascular access dysfunction [1–5], there has recently been a concerted attempt to increase the incidence and prevalence rate of successful arteriovenous (AV) fistulae in the hemodialysis population [6–10]. While this is an important step in the right direction, it has resulted in reported rates of fistula non-maturation (early AV fistula failure) that vary between 23% and 50%, both in the United States [10–14] and in Europe [15], despite guidelines to optimize AV fistula placement and maturation [8]. The reasons for non-maturation are not clearly understood [16,17], but are thought to be due to a combination of (i) an inability of the vein and artery to dilate appropriately in response to increased flow and (ii) possibly an exaggerated neointimal response [18]. In addition to initial non-maturation, AV fistulae can also develop a later (after 3 months) stenosis of the venous segment, which is characterized by neointimal hyperplasia [19]. Thus, although AV fistulae are the preferred form of

Correspondence to: Prabir Roy-Chaudhury MD, PhD, Division of Nephrology, University of Cincinnati, MSB G-251, 231, Albert Sabin Way, Cincinnati OH 45267-0585, USA.
Email: Prabir.roychaudhury@uc.edu
*Parts of this work have been presented in abstract form at the ASAIO Annual Conference, Chicago, June 2006 and at the American Society of Nephrology Annual Meeting, San Diego, November 2006.

permanent dialysis access, we are still some distance away from the dream of being able to place a fistula that can support haemodialysis in every patient with end-stage renal disease (ESRD), regardless of anatomic, demographic or logistical restraints [20]. The aims of the current study, therefore, were to (i) develop and validate a pig model of AV fistula stenosis and (ii) use this model to identify cellular mechanisms involved in AV fistula failure, in order to develop and test out future novel therapies for this condition.

Methods

Animals

Four-month old, 50 kg Yorkshire Cross domestic swines were purchased from Yeazel and Co. (Wolverton, OH, USA) and kept in standard animal care facilities at the University of Cincinnati Medical Center.

Surgery

Pigs were anaesthetized and intubated with a combination of xylazine, telazol and atropine. Isoflurane was used for maintenance anaesthesia. Following standard surgical cleansing, a 6-inch skin incision was made just below the inguinal ligament. Fascial and muscle planes were carefully dissected out with attention to haemostasis. The femoral artery (usually about 4 mm) and vein (usually about 6 mm) were identified and dissected out bilaterally. The vein and artery were sized to ensure that there would not be stretching or kinking of the vein following creation of the AV fistula. All visible tributaries of the femoral vein were ligated. The femoral vein was then cut and ligated distally. The cut vein was trimmed so that the size of the venous mouth was ~1 cm. An arteriotomy was then made in the femoral artery and the femoral vein was anastomosed to the femoral artery using 6/0 polypropylene suture. Due to surgical and other issues the curve of the created AV fistula varied between approximately 30 and 90 degrees in different animals. Vessel loops were then released and a special emphasis was made to obtain excellent haemostasis. Special attention was paid to ensure that there was no kinking or torsion of the completed fistula. The fascia and skin were then closed in layers using 3/0 dexon and silk. Subcutaneous buprenorphine and fentanyl patches were used for peri- and post-operative analgesia as needed. All pigs were administered aspirin EC 325 mg from day-1 to the time of sacrifice, together with intra-operative heparin in a dose of 200 mg/kg every 2 h from the time of the first arteriotomy till the end of surgery. AV fistula patency was confirmed by auscultation immediately after surgery and then every 3 days.

Study design

Ten pigs were utilized in this validation study and a total of 16 fistulae were evaluated. Pigs were sacrificed at 2 days (four fistulae from two pigs), 7 days (three fistulae from two pigs), 28 days (three fistulae from two pigs) and 42 days (six fistulae from four pigs) time points. One fistula in the 28-day group and two in the 42-day group was lost due to thrombosis and these were excluded from the study. Neointimal hyperplasia was present in one of the animals which thrombosed after 20d. This animal was not included in the analysis due to the confounding effects of thrombosis on neointimal hyperplasia. One pig in the 7-day group had only one fistula placed.

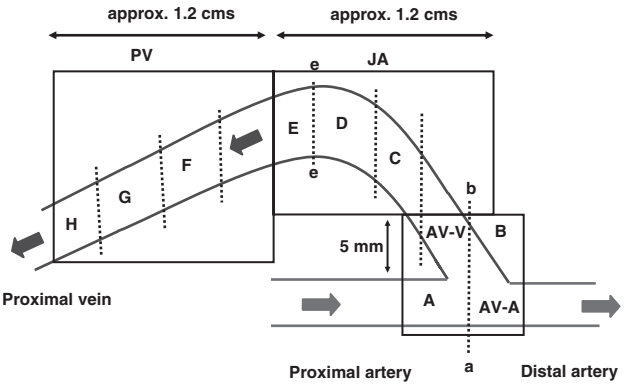

Fig. 1. Diagrammatic representation of AV fistula. The figure describes the division of the AV fistula into four different regions with capital letters indicating separate tissue blocks with the corresponding lower case letters (e–e for example) indicating the sites at which the tissue specimen was cut. The four main regions (indicated by the drawn rectangles) are the proximal vein (PV, blocks F–H), the juxta-anastomotic segment (JA, blocks C–E), the venous portion of the AV anastomosis (AV-V, block B) and the arterial portion of the AV anastomosis (AV-A, block A). Note that for the arteriovenous anastomosis, there is a combined block A+B that will be cut in the plane a–b, following which the artery (block A) and the vein (block B) are assessed separately.

Harvest, specimen preparation and terminology

At the time of sacrifice the animals were given a lethal injection of sodium pentothal and the entire AV fistula was removed *en bloc* and placed in formalin. The fistula was then carefully dissected out the same day to obtain ~3 cm of the venous segment, 3 cm of proximal artery and if possible 3 cm of distal artery (Figure 1). For the purpose of the current study, we will be focusing only on the AV anastomosis and the venous segment. The entire specimen was then allowed to fix in formalin for 48 h, following which it was coated in paraffin and sectioned as described in Figure 1. For the purpose of this study, the arterial and venous cross sections obtained by sectioning at the a–b level were analysed separately as the arterial (AV-A) and venous (AV-V) portions of the AV anastomosis. Following this, the remaining 2.5 cm (approximately) of the venous segment was cut into 4 mm blocks (blocks C–H in Figure 1). The first three 4 mm blocks following the AV anastomosis were considered to be the juxta-anastomotic (JA) segment (based on the classification by Beathard *et al.* [21] that described JA lesions as those immediately adjacent to the arterial anastomosis), with the next three blocks considered to be the proximal vein (PV). Thus, in Figure 1, block A + B would be considered to be from the arterial and venous sides of the AV anastomosis, respectively, blocks C to E from the JA segment and blocks F to H from the proximal vein. While we recognize that such divisions are sometimes arbitrary, we felt that the curved portion of the AV fistula should be within the JA segment. It is important to emphasize that the proximal vein in our classification refers only to vein between ~1.5–3 cms beyond the AV anastomosis. This is different from the generally accepted clinical view of the proximal vein

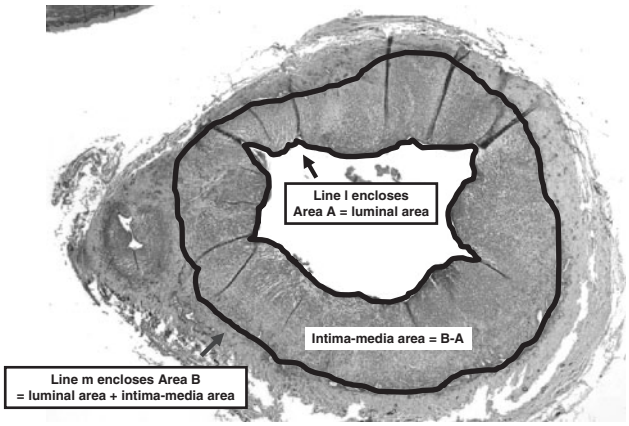

Fig. 2. Morphometric analyses. The morphometric analyses that were performed is described in the figure. Line 'l' encloses area A, which is the luminal area. Line 'm' encloses area B, which is the combined luminal + intima-media area. Luminal stenosis was defined as $A/B \times 100$. Intima-media area per unit length was defined as $(B-A)/L$. The specimen shown is a section of proximal vein at 42 days stained with an antibody to α-smooth muscle actin (SMA).

which would extend from the JA region to the central venous system. Three micron thick paraffin-embedded sections were then cut on a microtome and used for the histological, morphometric and immunohistochemical analyses.

Histology and immunohistochemistry

Sections from each region (for each specimen) were assessed with a haematoxylin and eosin stain and also for the expression of α-smooth muscle actin (SMA, a smooth muscle cell and myofibroblast marker: Dako, 1A4, 1: 100), desmin (a marker of differentiated contractile smooth muscle cells, Dako, DE-R-11, 1 : 200), vimentin (present on fibroblasts and myofibroblasts but not on contractile smooth muscle cells, Dako, Vim3B4, 1 : 200) and BrDU (a marker of cellular proliferation, Vector, 85-2C8, 1 : 400) using a standard streptavidin biotin immunohistochemical technique. Briefly, following deparaffinization and hydration, slides were washed and underwent protease digestion (if required for a particular primary antibody). Slides were then incubated with the primary antibody for 1 h with the biotinylated secondary antibody blend (anti-rabbit Ig, anti-mouse IgG and anti-mouse IgM blend, Vector Laboratories, Burlingame, CA, USA) for 30 min and with streptavidin/horseradish peroxidase for 30 min. All incubations were performed at room temperature with appropriate washes between each step. The slides were then developed with a diaminobenzidine/hydrogen peroxide mixture for 4 min, counterstained with haematoxylin, dehydrated with graduated alcohol and xylene, and mounted using a xylene-based medium. A brown colour indicated a positive stain. Negative controls were performed on each run, by substituting the primary antibody with PBS. In addition, positive control tissue (gut, lymph node and spleen) was used to document the efficacy of each antibody.

Histomorphometric analysis

One section each, from blocks A–H (from all the specimens) underwent a histomorphometric analysis for the measurement of (i) percentage luminal stenosis (%LS) and (ii) intima-media area per unit length (IMA/L). We divided the intima-media area by the circumference of the lumen, in order to correct for the degree of dilatation. Digital H and E and SMA stained pictures of one section from each block (A–H in Figure 1) were taken at a final magnification of 20x using an Olympus BH-2 microscope, a Sony chip camera and a Unix work station. Image J software was used for the morphometric analyses (see Figure 2). Percentage LS was calculated by drawing a line around the abluminal border of the intima-media (line m, Figure 2), followed by a line around the lumen (line l in Figure 2). The area subtended by line 'm' was defined as Area B (intima-media + luminal area), while the area subtended by line 'l' was defined as Area A (luminal area). Percentage stenosis was then calculated using the formula $A/B \times 100$ (Figure 2). The IMA was then calculated by subtracting the luminal area A from the intima-media + luminal area B (i.e. IMA = B–A in Figure 2). In addition, the intima media area (B–A) was divided by the luminal circumference (line l) to obtain the value for IMA/L. An average value for each region [PV, JA, AV-V and the arterial portion of the AV anastomosis (AV-A)], at each of the different time points was obtained for each specimen. Thus, the value for percentage LS for PV for the single specimen depicted in Figure 1, would be the average of the percentage LS for blocks F–H. The values for percentage LS for all the specimens from a specific region (PV for example) at a particular time point (six specimens for the 42-day time point) were then combined to get a mean +/− SE percentage LS for PV at that specific time point. A similar process was repeated for IMA/L at each time point. The intima and the media were considered to be a single entity, since in most cases it was impossible to clearly identify an internal elastic lamina. There was also in most cases no real difference at a histological level that would have allowed us to differentiate the neointima from the media.

Table 1. Statistical analysis of differences in percentage luminal stenosis and intima-media area per unit length between the 2 day and 42 days samples in different AV fistula regions

Percentage luminal stenosis (site)	*P*-value	Intima-Media Area per unit Length (site)	*P*-value
PV (0 *vs* 71%)	<0.0001	PV (3 *vs* 104)	<0.0001
JA (0 *vs* 62%)	<0.0001	JA (6 *vs* 85)	<0.0001
AV-V (0 *vs* 22%)	0.0002	AV-V (4 *vs* 23)	NS
AV-A (0 *vs* 6%)	NS	AV-A (4 *vs* 5)	NS

The 2-day value is given first (see Figure 3 for standard errors). PV, proximal vein; JA, juxta-anastomotic segment; AV-V, venous portion of the AV anastomosis; and AV-A, arterial portion of the AV anastomosis.

Statistics

An analysis of variance (ANOVA) analysis was used to identify differences between the same region of the AV fistula at different time points and between different regions at the same time point. A *P*-value of < 0.05 was considered to be statistically significant. Data are presented in Table 1 for differences between the same region at 2 days and 42 days (for example, a comparison of LS of PV at 2 days *vs* 42 days) and in Table 2 for differences between different regions of

Table 2. Statistical analysis of differences in percentage luminal stenosis and intima-media area per unit length between different AV fistula regions at the 42-day time point (see Figure 4 for standard errors)

Percentage luminal stenosis (comparator)	*P* value	Intima-media area per unit length (comparator)	*P* value
PV (71%) *vs* JA (62%)	0.051, NS	PV (104) *vs* JA (85)	0.218, NS
PV (71%) *vs* AV-V (22%)	<0.0001	PV (104) *vs* AV-V (23)	<0.0001
PV (71%) *vs* AV-A (6%)	<0.0001	PV (130) *vs* AV-A (5)	<0.0001
JA (62%) *vs* AV-V (22%)	<0.0001	JA (85) *vs* AV-V (23)	<0.0009
JA (62%) *vs* AV-A (6%)	<0.0001	JA (85) *vs* AV-A (5)	<0.0001
AV-V (22%) *vs* AV-A (6%)	0.004	AV-V (23) *vs* AV-A (5)	0.351, NS

PV, proximal vein; JA, juxta-anastomotic segment; AV-V, venous portion of the AV anastomosis; V-A, arterial portion of the AV anastomosis.

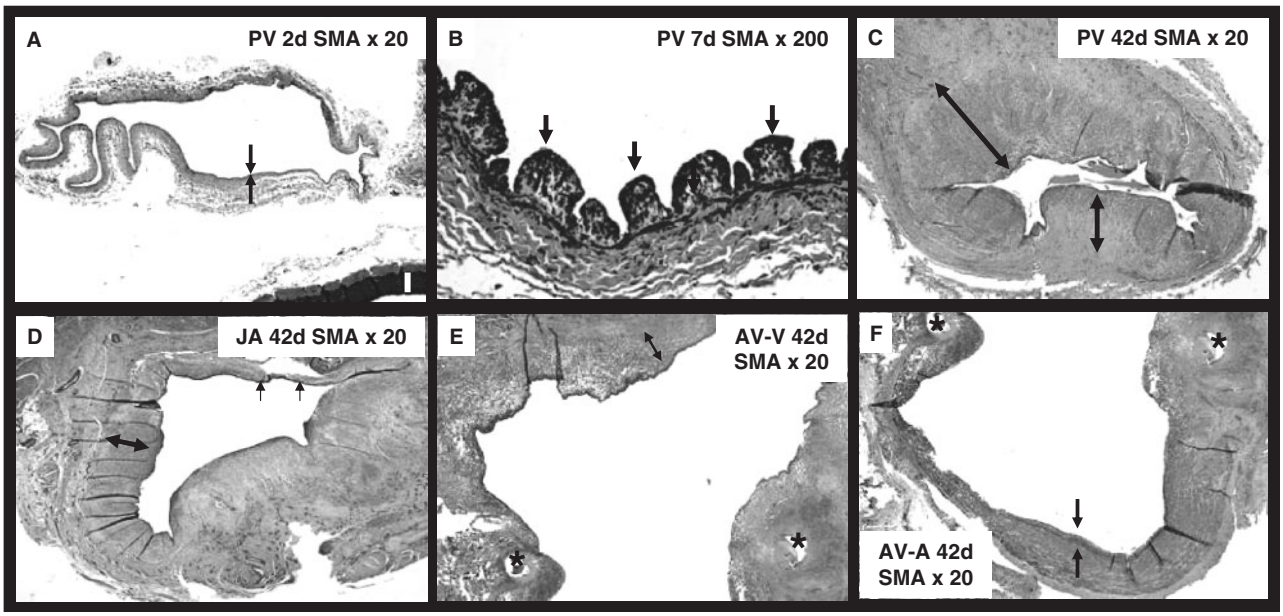

Fig. 3. Descriptive histology at different time points (**A**–**C**) and within different regions at the same time point (**C**–**F**): (**A**) shows the complete lack of intima-media thickening within the proximal vein (PV) at 2 days (the vessel wall is the region between the two arrows). By 7 days, the PV has developed bud like protuberances (**B**, arrows) and by 42 days these protuberances have coalesced, to result in a very significant degree of intima-media thickening (double-headed arrows) and luminal stenosis. (**D**) documents significant intima-media thickening (double-headed arrow) in the juxta-anastomotic (JA) region, albeit in an eccentric pattern (minimal thickening at the site of arrowheads). (**E**) and (**F**), demonstrate lesser degrees of intima-media thickening and neointimal hyperplasia at the venous (AV-V; **E**) and arterial (AV-A; **F**) portions of the AV anastomosis. The double arrow in (**E**) documents the magnitute of intima-media thickening within the vein, while the two arrows do the same for the artery in (**F**). Note that (**E**) and (**F**) are different parts of the same section in the plane a–b (Figure 1). The asterisks denote the common surgical suture sites.

the AV fistula at 42-days only (for example, a comparison of LS between the PV and the venous portion of the AV anastomosis at 42 days).

Results

Descriptive histology

Different time points. Figure 3 describes the progression of intima-media thickening in this model. At 2 days (Figure 3A), the entire intima-media is only about 3–4 cell layers thick as would be expected in normal vein. By 7 days, some of the venous specimens develop multiple buds in the PV and JA segments (Figure 3B). These buds then grow in size and coalesce together to result in the very significant degree of intima-media thickening present at 42 days (Figure 3C and D).

Different regions at the same time point. There appeared to be a marked increase in the degree of intima-media thickening at the 42-day time point, from the arterial end of the AV anastomosis to the PV. This is most apparent in the histomorphometric analyses (Figure 4A and B), but Figure 3C and F also emphasize this point, with significant intima-media thickening within the PV (3C) and JA segment (Figure 3D) as compared to relatively much less thickening within the venous and arterial portions of the AV anastomosis (Figure 3E and F, respectively). Interestingly, some sections of the PV and JA segment

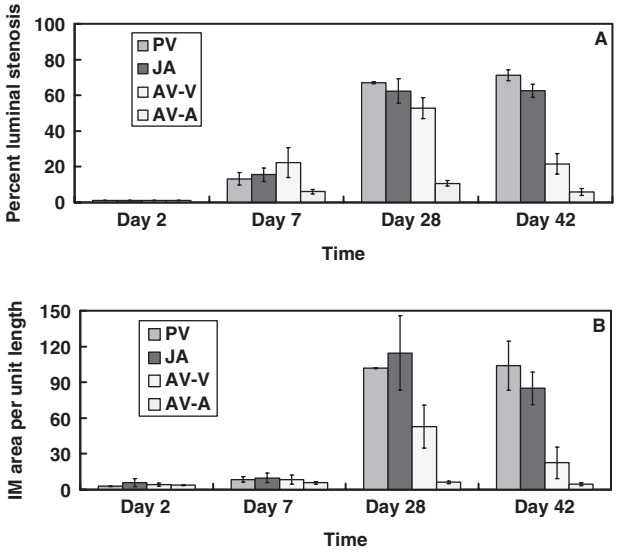

Fig. 4. Histomorphometric analyses. (**A**) describes the degree of luminal stenosis within different regions of the AV fistula at different time points. (**B**) does the same for intima-media area per unit length. Note that in general (with some biological variation), the degree of luminal stenosis and intima-media thickness per unit length increases from day 2 to day 42 and also increases from the arterial end of the AV anastomosis (AV-A) to the proximal vein (PV) at the 28-day and 42-day time points. (PV, proximal vein; JA, juxta-anastomotic segment; AV-V, venous portion of the AV anastomosis; AV-A, arterial portion of the AV anastomosis).

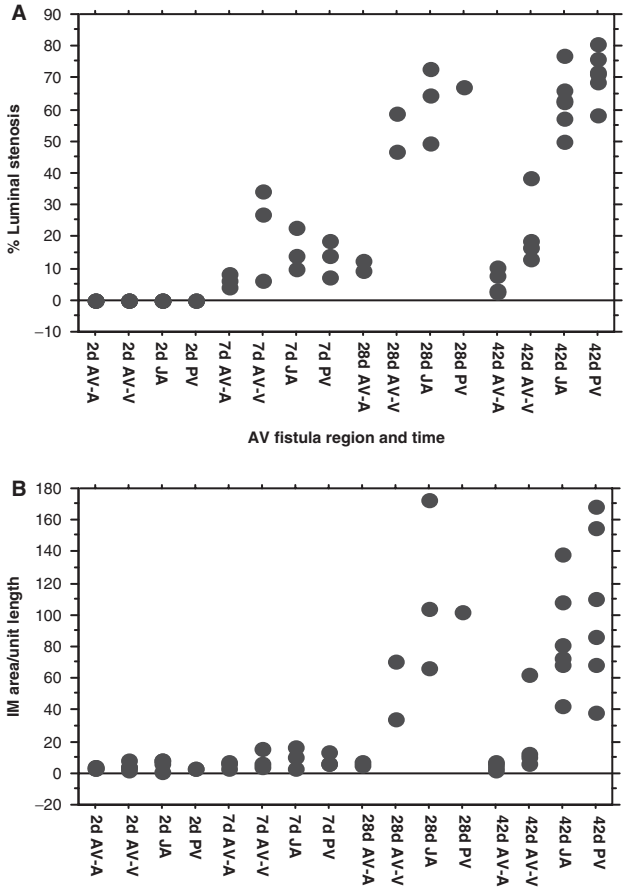

Fig. 5. Scattergrams for luminal stenosis (**A**) and intima-media thickening (**B**) for individual specimens at different time points. As in all biological systems there is a degree of biological variation between different animals and also between paired AV fistulae in the same animal. This variation appears to be more pronounced for intima-media thickening per unit length as compared to luminal stenosis.

demonstrated a very eccentric pattern of intima-media thickening, with a 40–50 cell layer thickness on one side of the vascular cross section as compared to a complete absence of neointimal hyperplasia on the opposite side of the same cross section (Figure 5E and F).

Histomorphometric analysis

Figure 4A and B summarize the changes in LS and IMA/L of the lumen circumference. Note that (i) the amount of luminal stenosis and intima-media thickening per unit length, tends to increase in a temporal fashion from 2 days to 42 days and (ii) at the 28-day and 42-day time points, LS and intima-media thickening tends to be far less within the AV anastomosis as compared to the JA and PV regions. Tables 1 and 2 summarize the actual values and the statistical analyses for the comparisons between the 2-day and 42-day time points in the different regions (Table 1) and for the comparisons between the different regions at the 42-day time point (Table 2) for both percentages of LS and IMA/L. Note that that the 28-day and 42-day values for both LS and intima-media thickening are significantly greater (Table 1; $P < 0.0001$) as compared to the 2-day and 7-day specimens. Similarly, LS and intima-media thickening are much more pronounced within the PV and JA segments in the 42-day specimens as compared to specimens from the AV anastomosis at the same 42-day time point (Table 2; $P < 0.0001$). Interestingly, the venous portion of the AV anastomosis has a significantly greater degree of luminal stenosis as compared to the arterial portion of the AV anastomosis.

Cellular phenotyping

Figure 5 describes representative sections from the proximal vein at 42 days that have been stained with antibodies against SMA, desmin and vimentin. Table 3 describes how these antibodies can be used to identify different cell types. The vast majority of cells within the region of intima-media thickening appear to be SMA-positive, vimentin-positive and desmin-negative cells, suggesting that they are myofibroblasts [22]. Of note there are a few desmin-positive cells (Figure 3D) within the region of intima-media thickening, which could be contractile smooth muscle cells. Perhaps the most interesting result from our immunohistochemical studies came from the analysis of BrdU staining in cross sections with eccentric intima media thickness. Thus, Figure 4F documents an impressive amount of endothelial cell (arrow) and myofibroblast (arrowhead)

proliferation on the side with intima-media thickening as compared to an almost complete absence of cellular proliferation on the side with minimal intima-media thickening (asterisk).

Discussion

We have described for the first time, the early histological changes that occur within different regions of the venous segment of a pig AV fistula at different time points following the creation of an AV fistula. We believe that this information about the temporal pattern of intima-media thickening, within different regions of the same AV fistula is an important addition to the already available information on the development of venous stenosis following the creation of a pig AV fistula [22, 23]. The results from our studies clearly document that (i) venous stenoses are maximal at specific sites within the venous segment (ii) intima-media thickening plays an important role in the pathogenesis of this early venous stenosis and (iii) the predominant cell type within the areas of venous stenosis is the myofibroblast. We believe that this work has special relevance in the current clinical climate of an increasing incidence of early AV fistula failure in that it both (i) identifies potential mechanisms for AV fistula failure and (ii) provides us with a clinically appropriate model for testing out new therapeutic interventions. Specific aspects of the current study are discussed subsequently.

Table 3. Cellular phenotyping of cells within the region of intima-media thickening in the pig, AV fistula model

	SMA	Vimentin	Desmin
Contractile SMCs	+	−	+
Myofibroblast	+	+	−
Fibroblast	−	+	−

Contractile smooth muscle cells are desmin + ve, SMA + ve and vimentin –ve; myofibroblasts are desmin –ve, SMA + ve and vimentin + ve; fibroblasts are desmin –ve, SMA –ve and Vimentin + ve.

Similarities to the human lesion

We have recently demonstrated the presence of aggressive and early neointimal hyperplasia in dialysis patients with AV fistula maturation failure [18]. This is in keeping with the finding of aggressive intima-media thickening in our pig model of AV fistula stenosis. In addition, as can be seen in Figure 6, the overall histological pattern of neointimal hyperplasia in dialysis patients with AV fistula failure [24] (Figure 6A) is very similar to that in our pig model (Figure 6B). This includes an eccentric distribution of the neointimal hyperplasia/intima-media thickening (compare Figure 6A to Figure 5E). The one partial exception is that stenotic human AV fistulae have a

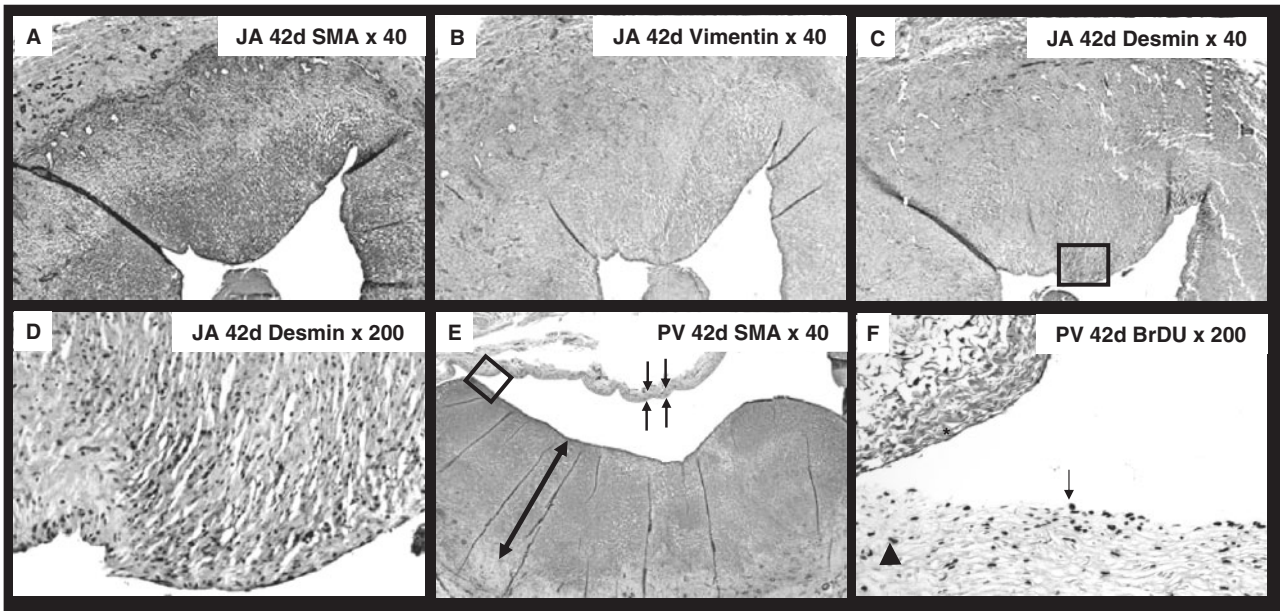

Fig. 6. Immunohistochemical analyses. The expression of smooth muscle alpha actin (**A**), vimentin (**B**) and desmin (**C**) within the same section from the juxta-anastomotic segment at 42 day can be seen. Note that the vast majority of cells are SMA and vimentin + ve but desmin −ve, suggesting that intima-media thickening in this AV fistula model is primarily made up of myofibroblasts. A high power view of (**C**) (rectangle), however, does show some desmin + ve cells within the region of intima-media thickening (**D**). (**E**), once again emphasizes the eccentric nature of the intima-media thickening (double headed arrow denotes significant intima-media thickening on one side as compared to the tissue between the two sets of black arrows (minimal thickening) on the other side). (**F**) is a high power view of the region within the rectangle in (**E**) which has been stained for BrDu (a marker for proliferating cells). Note the large number of proliferating cells [endothelial (arrow) and possible myofibroblasts (arrowhead)] on the side that has the intima-media thickening, as compared to almost no cell proliferation on the side with no intima-media thickening (asterisk) see new position of asterisk.

better developed medial layer in most cases, while our pig model samples were characterized primarily by combined intima-media thickening rather than separate medial and neointimal hyperplasia.

Variations in the magnitude of stenosis within the AV anastomosis and the venous segment

A key finding of our study was the very significant differences in intima-media thickening and luminal stenosis within different regions of the AV anastomosis and venous segment. Although haemodynamic measurements have not been described in this work, we believe that the described differences in the pattern of stenosis could be due to different patterns of haemodynamic stress in different regions of the AV fistula [25]. Also, in keeping with some of the previously published literature, the venous portion of the AV anastomosis tended to have more percentage stenosis and intima-media thickening (albeit not statistically significant for the latter), as compared to the arterial portion. While this could be due to the orientation of the venous jet flow, it could also be a manifestation of an exaggerated response to injury within the vein as compared to the artery.

In order to perform a detailed study of possible linkages between haemodynamic stress and histological change, however, it is essential to first develop a validated animal model that describes the temporal course of histological changes within different regions of the AV fistula. In this context, while previous large animal models of AV fistulae have been described in the goat [26] and in the pig [23], they have focused primarily on a single temporal end point, which has in most cases assessed changes only at the AV anastomosis [23], rather than within the venous segment, which is the true correlate of the clinical problem of AV fistula failure.

Advantages and disadvantages of the pig model

While considerable work has been performed on AV fistula models in small animals such as rodents and rabbits [27–30], these models (although excellent for detailed molecular analyses) are not ideal for intravascular flow studies, such as those that are often needed, in order to develop a complete haemodynamic shear stress profile. In particular, an assessment of the relative contributions of inadequate dilatation *vs* intima-media thickening and neointimal hyperplasia towards AV fistula stenosis can only be teased out in large animal models such as the one we have described (through the use of sophisticated imaging and histological techniques). Large animal models are also essential to identify the impact of different anatomical configurations of the AV fistula on haemodynamic shear stress profiles and AV fistula maturation and stenosis. Finally, local therapeutic interventions, such as endovascular or perivascular drug delivery, aimed at enhancing AV fistula maturation (dilatation) and minimizing intima-media thickening, can only be carried out in large animal models.

While other authors have described large animal models of arteriovenous graft and fistula stenosis in goats, dogs and sheep [26,31,32], we have previously emphasized the reasons for using the pig as the animal species of choice for the study of vascular stenosis [33]. These include (i) similarities in the vascular response to injury between pigs and humans; specifically, a direct correlation between the magnitude of vascular injury and the amount of neointimal hyperplasia [34], (ii) adequate development of neointimal hyperplasia over a short period, in contrast to dog AV stenosis models where stent placement may be required to develop stenosis [35], (iii) widespread use of the pig as a large animal model in coronary stenosis studies, (iv) lack of bone formation within the region of neointimal hyperplasia for both pigs and humans as opposed to a published sheep model of AV graft stenosis [32] and (v) recent advances in the mapping of the pig genome, which is likely to result in an increased number of molecular probes for use in pig studies (see the web site of the US Pig Genome Mapping Project at http://www.animalgenome.org/pig/). Finally, our emphasis on the use of the pig as the large animal model of choice for the study of arteriovenous stenosis is supported by published work from our group and others (Rotmans *et al.*) on the successful use of interventions to block arteriovenous stenosis in pig models [36–40].

It is important to mention, however, that the current model does have some potential drawbacks with regard to its potential future use to (i) elucidate the pathobiology of AV fistula failure and (ii) test out novel therapies for AV fistula failure. Specifically, our pigs are not uraemic [41] and we have not performed cannulation of our AV fistulae. Despite this, as noted earlier, the histological pattern of intima-media thickening in our pig model is very similar to that which occurs in the setting of dysfunctional human AV fistulae (Figure 6), albeit with a more defined media in the human samples. We believe that this emphasizes the fact that the biology of our animal model closely mirrors that of the human lesion and that the described model could be ideally suited for testing out interventions aimed at reducing the clinical burden associated with AV fistula failure. We also note that there is a degree of biological variation between different pigs and AV fistulae at the same time point (Figure 7A and B). While it would ideal to be in a position to perform a histological analysis on the same animal at different time points, this is clearly not possible at a practical level. However, we believe that (i) the consistent trends (increase or decrease) shown by our data, both in the context of different AV fistula regions at the same time point (Table 2) as also for the same AV fistula region at different time points (Figure 1) and (ii) the fact that these trends achieved statistical significance suggest that the model that we have described could be used to for future mechanistic and interventional studies.

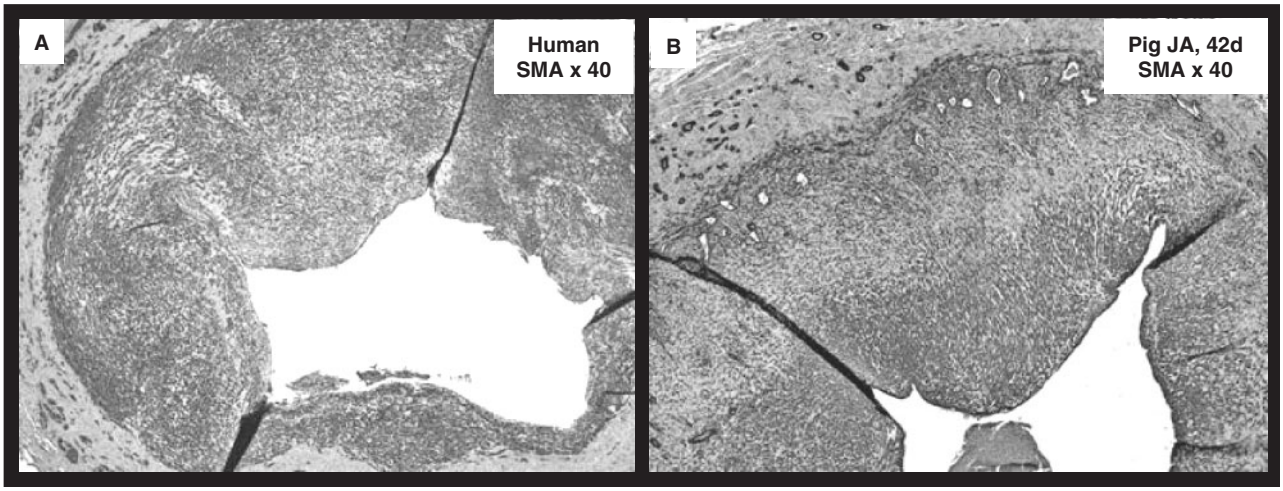

Fig. 7. Comparison of pig and human AV fistula stenosis. (**A**) demonstrates neointimal hyperplasia comprised of SMA positive cells in a dysfunctional human AV fistula that never matured adequately for use, while (**B**) documents a very similar pattern of SMA positive cells in a specimen from the JA segment of our pig AV fistula model, 42 days post-surgery. Note also the eccentric distribution of vascular stenosis within a single cross section of the human specimen (**A**), which is very similar to Figure 5E in the pig model.

Myofibroflasts are the predominant cell type responsible for AV fistula failure

As described in the Results section, the predominant cellular phenotype within the region of intima-media thickening is not the contractile smooth muscle cell but rather a vimentin-positive, SMA-positive, desmin-negative myofibroblast. This finding is in keeping with our own studies in dialysis patients that have documented the myofibroblast as the major cell type within the stenotic venous segment of dysfunctional AV fistulae and polytetrafluoroethylene (PTFE) grafts [24]. These data suggest that novel therapeutic interventions that target myofibroblast specific molecules, may be particularly effective in the clinical setting of dialysis access dysfunction.

In conclusion, we have developed and validated a pig model of AV fistula stenosis that appears to be very similar to the human lesion, with regard to the sites of stenosis, the cellular phenotype of the cells within the stenosis and the overall histological pattern of the stenosis. We believe that this study is unique, in that it (i) draws attention to the different histological patterns that are present within different regions of the AV fistula, at different time points following fistula creation (ii) describes animal model data that could be used to dissect out possible linkages between haemodynamic shear stress and AV fistula maturation/stenosis (iii) identifies the predominant cellular phenotype involved in AV fistula stenosis and (iv) provides the dialysis access community with a reliable large animal model that could be used to develop and test out novel therapies to address the current recalcitrant clinical problem of AV fistula stenosis.

Acknowledgements. This work has been supported by NIH grant R0-1 DK061689 and by a Satellite Dialysis Grant to Prabir Roy-Chaudhury.

Conflict of interest statement. None declared.

References

1. Feldman HI, Kobrin S, Wasserstein A. Hemodialysis vascular access morbidity. *J Am Soc Nephrol* 1996; 7: 523–535
2. Egger P. *Trends in Medicare Expenditure for Vascular Access*. Cincinnati Hemodialysis Vascular Access Symposium 2004, Cincinnati, OH, USA
3. McCarley P, Wingard RL, Shyr Y, Pettus W, Hakim RM, Ikizler TA. Vascular access blood flow monitoring reduces access morbidity and costs. *Kidney Int* 2001; 60: 1164–1172
4. Roy-Chaudhury P, Sukhatme VP, Cheung AK. Hemodialysis vascular access dysfunction: a cellular and molecular viewpoint. *J Am Soc Nephrol* 2006; 17: 1112–1127
5. Roy-Chaudhury P, Kelly BS, Melhem M *et al*. Vascular access in hemodialysis: issues, management, and emerging concepts. *Cardiol Clin* 2005; 23: 249–273
6. Beasley C, Rowland J, Spergel L. Fistula first: an update for renal providers. *Nephrol News Issues* 2004; 18: 88–90
7. Beathard GA. Strategy for maximizing the use of arteriovenous fistulae. *Semin Dial* 2000; 13: 291–296
8. DOQI. Vascular Access Guidelines. *Am J Kid Dis* 2006; 48: S177–S247
9. Hemphill H, Allon M, Konner K, Work J, Vassalotti JA. How can the use of arteriovenous fistulas be increased? *Semin Dial* 2003; 16: 214–223
10. Allon M, Robbin ML. Increasing arteriovenous fistulas in hemodialysis patients: problems and solutions. *Kidney Int* 2002; 62: 1109–1124
11. Patel ST, Hughes J, Mills JL, Sr. Failure of arteriovenous fistula maturation: an unintended consequence of exceeding dialysis outcome quality Initiative guidelines for hemodialysis access. *J Vasc Surg* 2003; 38: 439–445., discussion 45
12. Tordoir JH, Rooyens P, Dammers R, van der Sande FM, de Haan M, Yo TI. Prospective evaluation of failure modes in autogenous radiocephalic wrist access for haemodialysis. *Nephrol Dial Transplant* 2003; 18: 378–383
13. Dixon BS, Novak L, Fangman J. Hemodialysis vascular access survival: upper-arm native arteriovenous fistula. *Am J Kidney Dis* 2002; 39: 92–101
14. Oliver MJ, McCann RL, Indridason OS, Butterly DW, Schwab SJ. Comparison of transposed brachiobasilic fistulas

to upper arm grafts and brachiocephalic fistulas. *Kidney Int* 2001; 60: 1532–1539
15. Rooijens PP, Burgmans JP, Yo TI *et al*. Autogenous radial-cephalic or prosthetic brachial-antecubital forearm loop AVF in patients with compromised vessels? A randomized, multicenter study of the patency of primary hemodialysis access. *J Vasc Surg* 2005; 42: 481–486., discussions 7
16. Dixon BS. Why don't fistulas mature? *Kidney Int* 2006; 70: 1413–1422
17. Asif A, Roy-Chaudhury P, Beathard G. Early arteriovenous fistula failure: a logical proposal for when and how to intervene. *Clin J Am Soc Nephrol* 2006; 1: 332–339
18. Roy-Chaudhury P, Arend L, Samaha A *et al*. Aggressive early neointimal hyperplasia contributes to av fistula maturation failure. *Am J Kidney Disease* 2007; (In Press)
19. Stracke S, Konner K, Kostlin I *et al*. Increased expression of TGF-beta1 and IGF-I in inflammatory stenotic lesions of hemodialysis fistulas. *Kidney Int* 2002; 61: 1011–1019
20. Rooijens PP, Tordoir JH, Stijnen T, Burgmans JP, Smet de AA, Yo TI. Radiocephalic wrist arteriovenous fistula for hemodialysis: meta-analysis indicates a high primary failure rate. *Eur J Vasc Endovasc Surg* 2004; 28: 583–589
21. Beathard GA, Arnold P, Jackson J, Litchfield T. Aggressive treatment of early fistula failure. *Kidney Int* 2003; 64: 1487–1494
22. Johnson MS, McLennan G, Lalka SG, Whitfield RM, Dreesen RG. The porcine hemodialysis access model. *J Vasc Interv Radiol* 2001; 12: 969–977
23. Nugent HM, Groothuis A, Seifert P *et al*. Perivascular endothelial implants inhibit intimal hyperplasia in a model of arteriovenous fistulae: a safety and efficacy study in the pig. *J Vasc Res* 2002; 39: 524–533
24. Roy-Chaudhury P, Arend L, Zhang J *et al*. Cellular Phenotypes in Dialysis Access Stenosis: Myofibroblasts, Fibroblasts and Contractile Smooth Muscle Cells. *J Am Soc Nephrol* 2006; 17: 75A
25. Krishnamoorthy M, Wang Y, Zhang J *et al*. Hemodynamic Shear Stress Modeling and AV Fistula Stenosis in a Pig AV Fistula Model. *J Am Soc Nephrol* 2006; 17: 74A
26. Lemson MS, Daemen MJ, Kitslaar PJ, Tordoir JH. A new animal model to study intimal hyperplasia in arteriovenous fistulas. *J Surg Res* 1999; 85: 51–58
27. Tronc F, Mallat Z, Lehoux S, Wassef M, Esposito B, Tedgui A. Role of matrix metalloproteinases in blood flow-induced arterial enlargement: interaction with NO. *Arterioscler Thromb Vasc Biol* 2000; 20: E120–E126
28. Masuda H, Zhuang YJ, Singh TM *et al*. Adaptive remodeling of internal elastic lamina and endothelial lining during flow-induced arterial enlargement. *Arterioscler Thromb Vasc Biol* 1999; 19: 2298–2307
29. Castier Y, Brandes RP, Leseche G, Tedgui A, Lehoux S. p47phox-dependent NADPH oxidase regulates flow-induced vascular remodeling. *Circ Res* 2005; 97: 533–540
30. Nath KA, Kanakiriya SK, Grande JP, Croatt AJ, Katusic ZS. Increased venous proinflammatory gene expression and intimal hyperplasia in an aorto-caval fistula model in the rat. *Am J Pathol* 2003; 162: 2079–2090
31. Chen C, Lumsden AB, Ofenloch JC *et al*. Phosphorylcholine coating of ePTFE grafts reduces neointimal hyperplasia in canine model. *Ann Vasc Surg* 1997; 11: 74–79
32. Kohler TR, Kirkman TR. Dialysis access failure: A sheep model of rapid stenosis. *J Vasc Surg* 1999; 30: 744–751
33. Kelly BS, Heffelfinger SC, Whiting JF *et al*. Aggressive venous neointimal hyperplasia in a pig model of arteriovenous graft stenosis. *Kidney Int* 2002; 62: 2272–2280
34. Schwartz RS, Edwards WD, Bailey KR, Camrud AR, Jorgenson MA, Holmes DR,Jr. Differential neointimal response to coronary artery injury in pigs and dogs. Implications for restenosis models. *Arterioscler Thromb* 1994; 14: 395–400
35. Trerotola SO, Carmody TJ, Timmerman RD *et al*. Brachytherapy for the prevention of stenosis in a canine hemodialysis graft model: preliminary observations. *Radiology* 1999; 212: 748–754
36. Kelly B, Melhem M, Zhang J *et al*. Perivascular paclitaxel wraps block arteriovenous graft stenosis in a pig model. *Nephrol Dial Transplant* 2006; 21: 2425–2431
37. Kelly BS, Narayana A, Heffelfinger SC *et al*. External beam radiation attenuates venous neointimal hyperplasia in a pig model of arteriovenous polytetrafluoroethylene (PTFE) graft stenosis. *Int J Radiat Oncol Biol Phys* 2002; 54: 263–269
38. Rotmans JI, Velema E, Verhagen HJ *et al*. Matrix metalloproteinase inhibition reduces intimal hyperplasia in a porcine arteriovenous-graft model. *J Vasc Surg* 2004; 39: 432–439
39. Rotmans JI, Verhagen HJ, Velema E *et al*. Local overexpression of C-type natriuretic peptide ameliorates vascular adaptation of porcine hemodialysis grafts. *Kidney Int* 2004; 65: 1897–1905
40. Rotmans JI, Pattynama PM, Verhagen HJ *et al*. Sirolimus-eluting stents to abolish intimal hyperplasia and improve flow in porcine arteriovenous grafts: a 4-week follow-up study. *Circulation* 2005; 111: 1537–1542
41. Misra S, Gordon JD, Fu AA *et al*. The porcine remnant kidney model of chronic renal insufficiency. *J Surg Res* 2006; 135: 370–379

Received for publication: 8.1.07
Accepted in revised form: 18.7.07